Sequence Requirements of the ATP-Binding Site within the C-Terminal Nucleotide-Binding Domain of Mouse P-Glycoprotein: Structure−Activity Relationships for Flavonoid Binding[†]

Heidi de Wet,[‡] David B. McIntosh,*[,‡] Gwenaëlle Conseil,[§] Hélène Baubichon-Cortay,[§] Tino Krell,[§] Jean-Michel Jault,[§] Jean-Baptiste Daskiewicz,[||] Denis Barron,[||] and Attilio Di Pietro[§]

Department of Chemical Pathology, University of Cape Town Medical School, Observatory 7925, Cape Town, South Africa, Institut de Biologie et Chimie des Protéines, UMR 5086, CNRS/Université Claude Bernard-Lyon I, 7 Passage du Vercors, 69367 Lyon Cedex 07, France, and Laboratoire des Produits Naturels, UMR 5013, CNRS/Université Claude Bernard-Lyon I, 69622 Villeurbanne, France

Received April 2, 2001; Revised Manuscript Received June 1, 2001

ABSTRACT: Sequence requirements of the ATP-binding site within the C-terminal nucleotide-binding domain (NBD2) of mouse P-glycoprotein were investigated by using two recombinantly expressed soluble proteins of different lengths and photoactive ATP analogues, 8-azidoadenosine triphosphate ($8N_3$-ATP) and 2′,3′,4′-*O*-(2,4,6-trinitrophenyl)-8-azidoadenosine triphosphate (TNP-$8N_3$-ATP). The two proteins, Thr^{1044}−Thr^{1224} ($NBD2_{short}$) and Lys^{1025}−Ser^{1276} ($NBD2_{long}$), both incorporated the four consensus sequences of ABC (ATP-binding cassette) transporters, Walker A and B motifs, the Q-loop, and the ABC signature, while differing in N-terminal and C-terminal extensions. Radioactive photolabeling of both proteins was characterized by hyperbolic dependence on nucleotide concentration and high-affinity binding with $K_{0.5}$($8N_3$-ATP) = 36−37 μM and $K_{0.5}$(TNP-$8N_3$-ATP) = 0.8−2.6 μM and was maximal at acidic pH. Photolabeling was strongly inhibited by TNP-ATP (K_D = 0.1−5 μM) and ATP (K_D = 0.5−2.7 mM). Since flavonoids display bifunctional interactions at the ATP-binding site and a vicinal steroid-interacting hydrophobic sequence [Conseil, G., Baubichon-Cortay, H., Dayan, G., Jault, J.-M., Barron, D., and Di Pietro, A. (1998) *Proc. Natl. Acad. Sci. U.S.A. 95*, 9831−9836], a series of 30 flavonoids from different classes were investigated for structure−activity relationships toward binding to the ATP site, monitored by protection against photolabeling. The 3-OH and aromaticity of conjugated rings A and C appeared important, whereas opening of ring C abolished the binding in all but one case. It can be concluded that the benzopyrone portion of the flavonoids binds at the adenyl site and the phenyl ring B at the ribosyl site. The Walker A and B motifs, intervening sequences, and small segments on both sides are sufficient to constitute the ATP site.

Multidrug resistance (MDR[1]) is a common obstacle in successful treatment of cancer (*1*). Classical MDR is the phenomenon whereby cancer cells become resistant to a wide variety of structurally unrelated compounds with different subcellular targets, after prolonged exposure to a single compound. Overexpression of a 140−170 kDa protein, called P-glycoprotein (P-gp), is implicated in MDR (*2*). P-gp consists of two homologous halves, each made up of a transmembrane domain followed by a nucleotide-binding domain (NBD) on the cytoplasmic face of the membrane (*3*, *4*). The protein belongs to the large family of ABC (ATP-binding cassette) transporters, where different domain arrangements are found and where the domains may be separate proteins. The NBDs can be linked to other functional protein entities, creating a wide family of ABC ATPases.

The NBDs of ABC ATPases contain four sequence signatures: the Walker A [$G(X)_4GKS/T$] and Walker B [$R/K(X)_{6-8}L(Hyd)_4D$] motifs (*5*) and, in between, the ABC signature [$LSGG(X)_3R(Hyd)X(Hyd)A$] (*6*) and the Q-loop [$(Hyd)_2XQ$] (*7*), where Hyd indicates any hydrophobic amino

[†] This work was supported by grants and/or bursaries from the National Research Foundation of South Africa, the Paul and Stella Loewenstein trust, the Ethel and Ernst Erikson trust, FRD/CNRS agreements between D.B.M. and A.D.P., and Commité du Rhône de la Ligue Nationale Contre le Cancer; and the European Community (Polybind Project QLK1-1999-00505). G.C. and T.K. were recipients of fellowships from the Ligue Nationale Contre le Cancer (Commité de Haute-Savoie) and the European Union (TMR-Marie Curie ERBFMBIC972623), respectively.

* To whom correspondence should be addressed. Phone: +27-21-4066187. Fax: +27-21-4488150. E-mail: davidmci@chempath.uct.ac.za.

[‡] University of Cape Town Medical School.

[§] Institut de Biologie et Chimie des Protéines, CNRS/Université Claude Bernard-Lyon I.

[||] Laboratoire des Produits Naturels, CNRS/Université Claude Bernard-Lyon I.

[1] Abbreviations: ABC, ATP-binding cassette; DMA, dimethylallyl; EDTA, ethylenediaminetetraacetic acid; Ger, geranyl (=Pre_2); HECAMEG, 6-*O*-(*N*-heptylcarbamoyl)methyl-α-D-glucopyranoside; LDAO, lauryldimethylamine oxide; MDR, multidrug resistance; $8N_3$-ATP, 8-azidoadenosine triphosphate; NBD, nucleotide-binding domain; NBD1, N-terminal NBD; NBD2, C-terminal NBD; $NBD2_{long}$, mouse recombinant NBD2 from Lys^{1025} to Ser^{1276}; $NBD2_{short}$, mouse recombinant NBD2 from Thr^{1044} to Thr^{1224}; P-gp, P-glycoprotein; Pre, prenyl (=3,3-DMA); TNP-$8N_3$-ATP, 2′,3′,4′-*O*-(2,4,6-trinitrophenyl)-8-azidoadenosine triphosphate.

10.1021/bi010657c CCC: $20.00
Published on Web 08/03/2001

acid. P-gp shows a drug-stimulated, vanadate-inhibited, ATPase activity with a K_m for MgATP around 1 mM and a V_{max} of 0.3−2 (μmol/min)/mg of protein (*8*, *9*). While P-gp exhibits a low affinity for ATP, TNP-ATP binds approximately 1000-fold tighter (*10*−*12*). The photoactive ATP analogue $8N_3$-ATP labels conserved Tyr of hamster P-gp, positioned 26 residues before the Walker A motif (*13*). Vanadate trapping of ATP, chemical derivatization, and mutagenesis demonstrate that cooperativity between the N-terminal NBD (NBD1) and the C-terminal NBD (NBD2) is mandatory for ATPase activity (*14*−*20*). Mutagenesis, photolabeling, and competition studies place at least two drug transport sites in the transmembrane domains of the protein (*21*−*30*).

P-gp modulators are responsible for decreased drug extrusion and reversal of cellular multidrug resistance. Even though they are structurally divergent, they all are relatively hydrophobic. They competitively or uncompetitively inhibit efflux of cytotoxic agents from the cell (*31*−*33*). Allosteric inhibitory sites, distinct from the transport sites, appear to be present as well. Flavonoids, compounds prevalent in our diet, have been explored as reversal agents, and kaempferol, quercetin, and genistein have been demonstrated to modulate resistance, although apparently conflicting results have been obtained with different cancer cell lines (*34*−*36*). The flavonoid nucleus offers an attractive scaffold for substitutions in different directions, and a systematic study of *N*-benzylpiperazine derivatives showed that several compounds potentiated doxorubicin cytotoxicity on resistant cells (*37*).

The modular structure of ABC transporters suggests that P-gp function may be able to be reconstituted from separate NBDs and transmembrane domains. The study of isolated individual domains would greatly simplify the localization of drug- and reverser-binding sites, and a comparison of the properties of the isolated domains and the whole protein could shed light on the roles of each domain, the nature of noncovalent subunit interaction, and the coupling mechanism. Each individual half-molecule exhibits low ATPase activity, and drug-dependent stimulation requires the interaction of both halves (*38*). Recombinantly expressed mouse NBD1 and NBD2 bind nucleotides, and show very low or no ATPase activity (*10*, *12*). Certain flavonoids from different classes bind to isolated mouse NBD2 and partially inhibit nucleotide binding, suggesting overlapping sites (*39*). There is a correlation between the tightness of flavonoid binding to isolated NBD2 from the *Leishmania tropica* multidrug transporter and the degree of inhibition of daunomycin efflux from the parasite (*40*). However, hydrophobic prenylated flavonoids seem to exert their effect at the drug transport site rather than the ATP site in the yeast transporter Pdr5p (*41*).

In this study, we report the photolabeling of two recombinant NBD2 proteins of different lengths by $8N_3$-ATP and TNP-$8N_3$-ATP, and the binding of nucleotides and flavonoids. Both proteins contain the four consensus sequences typical of ABC ATPases, but the shorter one lacks a 19 amino acid segment on the N-terminal portion, including the tyrosine photolabeled by $8N_3$-ATP in hamster P-gp, and a 52 amino acid segment on the C-terminal end. Both proteins were efficiently derivatized by the two probes in a manner that suggested derivatization solely at the ATP site. This allowed us to define the requirements of flavonoid binding to the ATP site.

EXPERIMENTAL PROCEDURES

Materials. All buffers, imidazole, and Triton X-100 were from Sigma. HECAMEG was from Calbiochem, glycerol was from Carlo Erba or Sigma, ATP was from Boehringer Mannheim or Sigma, and TNP-ATP was from Molecular Probes or was synthesized (*42*). Natural or synthetic flavonoids were obtained as previously detailed (*39*, *41*, *43*−*47*). Ni-NTA agarose-25 was from Qiagen.

Proteins. The two recombinant C-terminal NBD2 polypeptides from mouse P-gp Mdr1b used in this study were expressed in *E. coli*. The sequences of the two polypeptides were from Thr^{1044} to Thr^{1224} ($NBD2_{short}$) and from Lys^{1025} to Ser^{1276} ($NBD2_{long}$). The proteins were expressed as N-terminal hexahistidine-tagged recombinant polypeptides.

Insertion in the pQE30 plasmid of the DNA encoding $NBD2_{short}$ and overexpression and purification of the recombinant protein were as previously described (*39*). The DNA encoding $NBD2_{long}$ was prepared from the recombinant pGEX-KT plasmid encoding the GST−NBD2 fusion protein where it had been inserted in *Bam*HI−*Eco*RI sites (*10*). After linearization by *Eco*RI, blunt ends were generated using Klenow fragments, and the DNA was digested by *Bam*HI, releasing only $NBD2_{long}$ DNA. After purification, the DNA was ligated between the *Bam*HI and *Sma*I sites of the pQE30 plasmid (Qiagen; containing the N-terminal hexahistidine-coding sequence), and used to transform JM109 *E. coli* cells. After induction with 1 mM isopropyl-1-thio-β-D-galactopyranoside for 3 h at 30 °C, cells were harvested by centrifugation and frozen at −80 °C. Cells were thawed and suspended in 50 mM Tris−HCl, 250 mM NaCl, 1 mM EDTA, 7 mM $MgCl_2$, 2% LDAO, 1.5 mM phenylmethylsulfonyl fluoride, 5 μM pepstatin, and 5 μM leupeptin, pH 7.5. After addition of benzonase, cells were lysed with a SLM-Aminco French cell press at 1000 psi; the lysate was 2-fold diluted with 40 mM NaPi, 20% glycerol, 900 mM NaCl, 50 mM imidazole, and 10 mM β-mercaptoethanol, pH 7.2, and centrifuged at 30000*g* for 30 min. The supernatant was incubated in batch with nickel-agarose previously equilibrated in 20 mM NaPi, 2% LDAO, 1 M NaCl, 25 mM imidazole, and 10% glycerol, pH 7.2. The solution was added to a column and the sedimented resin washed with 20 column volumes of 20 mM NaPi, 10% glycerol, 1.5% LDAO, 1 M NaCl, 30 mM imidazole, and 5 mM β-mercaptoethanol, pH 7.2. After several washes with increasing imidazole concentrations up to 70 mM, the protein was eluted with 20 mM NaPi, 25% glycerol, 0.3% β-octylglucoside, 250 mM imidazole, and 5 mM β-mercaptoethanol, pH 7.2. The protein was immediately transferred onto a column containing DEAE-Sepharose (Pharmacia) equilibrated with 20 mM NaPi, 25% glycerol, and 0.3% β-octylglucoside, pH 7.2, and the flow through collected since it contained purified $NBD2_{long}$. The eluate was finally dialyzed against 20 mM NaPi, 20% glycerol, 0.5 M NaCl, 0.01% HECAMEG, 1 mM EDTA, and 5 mM β-mercaptoethanol, pH 7.2. A typical yield of this procedure was 1.0−1.5 mg of pure protein/L of cell culture.

Photolabeling and SDS−*PAGE*. The standard irradiation medium for $NBD2_{short}$ and $NBD2_{long}$ was 25 mM buffer, 20%

(w/v) glycerol, and 0.01% (w/v) Triton X-100 in a volume of 75 or 100 μL. The buffer and pH, as well as conditions deviating from the standard, are specified in the captions to the figures.

Samples were irradiated using a 100 W xenon lamp (Hi-Tech) with quartz cuvettes of fresh toluene positioned at either side of the central quartz cuvette to protect the protein from ultraviolet radiation damage (cutoff at approximately 290 nm). Irradiated samples were transferred to Eppendorf tubes on ice, and 8 μL of 20% (w/v) SDS, containing trace amounts of bromophenol blue, was added. Samples were subjected to SDS−PAGE in 15% (w/v) polyacrylamide gels prepared according to Laemmli (*49*) and run for 3 h at 4 °C and 35 mA. Gels were dried and the radioactivity quantified using an Instant Imager (Packard Instrument Co.). Graphs were drawn using Sigma Plot 3.0 (Jandel Scientific Software). The data obtained from concentration-dependent photolabeling of proteins with [γ-^{32}P]TNP-8N$_3$-ATP or [γ-^{32}P]8N$_3$-ATP were fitted to the binding equation

$$Y = Y_{max}[S])/(K_{0.5} + [S])$$

where Y = relative counts, Y_{max} = relative maximum counts, [S] = nucleotide probe concentration, and $K_{0.5}$ = concentration of the probe at which half-maximal labeling is obtained.

Data obtained from ATP (or other inhibitor) inhibition of either [γ-^{32}P]TNP-8N$_3$-ATP or [γ-^{32}P]8N$_3$-ATP photolabeling were fitted to the binding algorithm

$$Y = \{100K_{0.5}(ATP)/(K_{0.5}(ATP) + [ATP])\} + F$$

where Y = percent photolabeling, F = offset, and $K_{0.5}$ = concentration of ATP at half-maximal inhibition.

The "true" dissociation constant for ATP (or other inhibitor) binding was obtained from the equation

$$K_D(ATP) = K_{0.5}(ATP)/\{1 + ([TNP\text{-}8N_3\text{-}ATP]/K_{0.5}[TNP\text{-}8N3\text{-}ATP])\}$$

where TNP-8N$_3$-ATP could also be 8N$_3$-ATP, depending on the radiolabel used.

The pK_a values for pH-dependent photolabeling of various proteins with [γ-^{32}P]TNP-8N$_3$-ATP or [γ-^{32}P]8N$_3$-ATP were obtained from the equation

$$Y = \{(A \times 10^{pK_a - x})/(10^{pK_a - x} + 1)\} + F$$

where Y = percent photolabeling, A = 100, x = pH, and F = offset.

Quantification of derivatization was performed by precipitating irradiated protein with a 13-fold excess of ice-cold 10% (w/v) trichloroacetic acid and collecting the protein on GF/F 2.5 cm Whatman filter paper with a mild vacuum. The filters were washed twice with 5 mL of 5% acid and assayed for radioactivity. Alternatively, the amount of radioactivity associated with the protein bands following SDS−PAGE and instant imaging was measured by reference to a known amount of a radioactive probe placed on small squares of filter paper and incorporated above and below the gel just before drying. The average radioactivity was used for quantification.

Synthesis of [γ-^{32}P]8N$_3$-ATP and [γ-^{32}P]TNP-8N$_3$-ATP. 8N$_3$-ATP and the high-affinity derivative TNP-8N$_3$-ATP were synthesized as described (*50*). High-specific-activity [γ-^{32}P]8N$_3$-ATP was prepared by an exchange method (*51*), and the TNP moiety was added as previously described (*52*).

Synthesis of 4′-Azido-5-hydroxy-7-[^{14}C]methoxyflavone. The starting compound, 376 mg of 5,5-dihydroxy-4′-nitroflavone (**1**), obtained according to ref *53*, was reduced to 4′-amino-5,7-dihydroxyflavone (**2**) by catalytic hydrogen transfer (*54*) in 50 mL of dry methanol, upon addition of 400 mg of ammonium formate and 100 mg of 10% Pd on activated carbon. The medium was stirred under argon for 22 h, the catalyst was removed by filtration and washed with methanol, and the filtrate was diluted with water and extracted with ethyl acetate. Purification of the extract on diol-bonded silica using a gradient of ethyl acetate in hexane yielded 231 mg (68% yield) of **2**: ^{1}H NMR (300 MHz, CDCl$_3$) δ = 13.19 (s, 1 H, OH-5), 7.80 (d, 2 H, J = 8.8 Hz, H-2′, H-6′), 6.82 (d, 2 H, J = 8.8 Hz, H-3′, H-5′), 6.54 (s, 1 H, H-3), 6.51 (d, 1 H, J = 2.1 Hz, H-8), 6.24 (d, 1 H, J = 2.1 Hz, H-6); ^{13}C NMR (75 MHz, CDCl$_3$) δ = 182.4 (C-4), 165.3 (C-7), 164.1 (C-2), 162.9 (C-5), 158.2 (C-9), 153.0 (C-4′), 128.4 (C-2′, C-6′), 118.6 (C-1′), 114.3 (C-3′, C-5′), 104.8 (C-10), 101.7 (C-3), 99.0 (C-6), 94.1 (C-8); positive high-resolution fast bombardment mass spectrometry [M + H] m/z 270.0770 (calcd for $C_{15}H_{12}NO_4$ 270.0766). The 4′-azido-5,7-dihydroxyflavone (**3**) was prepared according to ref *54* from 207 mg of **2** dissolved in 10 mL of 4 N aqueous HCl, cooled to 0 °C, and dropwise mixed with 8 mL of a solution of 266 mg of $NaNO_2$ in 15 mL of H_2O, so that the temperature never exceeded 5 °C. After 1 h of stirring at 0−4 °C, a solution of 500 mg of sodium azide in 10 mL of H_2O was added, dropwise, in the dark, and the medium stirred at room temperature for 1 h. The reaction was stopped by addition of ice and 10% aqueous $NaHCO_3$. Extraction with diethyl ether and purification of the extract on diol-bonded silica, using a gradient of ethyl acetate in hexane as solvent, furnished 214 mg (94% yield) of **3**: ^{1}H NMR (300 MHz, acetone-d_6) δ = 12.91 (s, 1 H, OH-5), 9.73 (s, 1 H, OH-7), 8.13 (d, 2 H, J = 8.8 Hz, H-2′, H-6′), 7.30 (d, 2 H, J = 8.8 Hz, H-3′, H-5′), 6.79 (s, 1 H, H-3), 6.58 (d, 1 H, J = 2.1 Hz, H-8), 6.29 (d, 1 H, J = 2.1 Hz, H-6); ^{13}C NMR (75 MHz, acetone-d_6) δ = 182.6 (C-4), 164.6 (C-7), 163.3 (C-2), 162.9 (C-5), 158.3 (C-9), 144.1 (C-4′), 128.6 (C-2′, C-6′), 128.3 (C-1′), 120.1 (C-3′, C-5′), 105.0 (C-10), 105.0 (C-3), 99.4 (C-6), 94.4 (C-8); positive high-resolution fast bombardment mass spectrometry [M + H] m/z 296.0678 (calcd for $C_{15}H_{10}N_3O_4$ 296.0671)]. The 4′-azido-5-hydroxy-7-methoxyflavone (**4**) was prepared from 11.3 mg of **3** in 1.5 mL of dimethylformamide to which 1.2 mg of tetrabutylammonium bromide, 7.9 mg of anhydrous K_2CO_3, and 3 μL of methyl iodide were added. After 1 h of reaction at room temperature with stirring, the reaction medium was diluted with water, acidified, and extracted with ethyl acetate. After filtration of the extract on a small column of silica gel using hexane−ethyl acetate (8:2) as solvent, 6.5 mg (55% yield) of **4** was recovered: ^{1}H NMR (300 MHz, CDCl$_3$) δ = 7.91 (d, 2 H, J = 8.9 Hz, H-2′, H-6′), 7.18 (d, 2 H, J = 8.9 Hz, H-3′, H-5′), 6.64 (s, 1 H, H-3), 6.51 (d, 1 H, J = 2.3 Hz, H-8), 6.40 (d, 1 H, J = 2.3 Hz, H-6), 2.19 (s, 3 H, CH_3); ^{13}C NMR (75 MHz, CDCl$_3$) δ = 182.7 (C-4), 166.0 (C-7), 163.4 (C-2), 162.6 (C-5), 158.1 (C-9), 144.2 (C-4′), 128.3 (C-2′, C-6′), 128.2 (C-1′), 120.0 (C-3′, C-5′), 106.0 (C-3), 105.3 (C-10), 98.6 (C-6), 93.1 (C-8), 30.1 (CH_3)]. For ^{14}C-

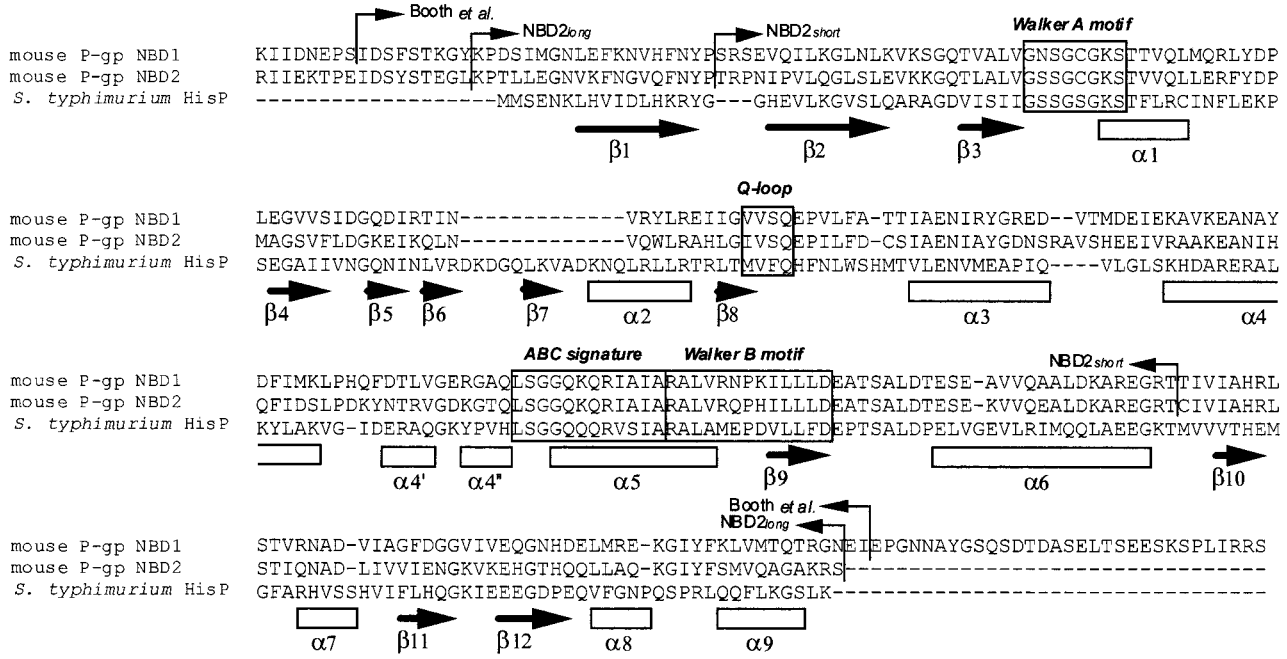

FIGURE 1: Alignment of the amino acid sequences of mouse P-gp NBD1 and NBD2 with that of bacterial HisP. The alignments were done with the ClustalW program. The secondary structural elements of HisP are derived from the high-resolution crystal structure (*56*). The limits of $NBD2_{short}$ and $NBD2_{long}$ are indicated, as well as those of the recombinant polypeptide of human NBD1 found to exhibit Mg^{2+}-dependent $8N_3$-ATP photolabeling (*57*). The four consensus sequences of ABC transporters are framed.

radiolabeled **4**, 85 μg of **3** was dissolved in 200 μL of dry dimethylformamide, and 9.3 μg of tetrabutylammonium bromide, 60 μg of anhydrous K_2CO_3, and 18 nmol of [^{14}C]-methyl iodide (1 mCi; 55 mCi/mmol) was added. After reaction for 1 h at room temperature with stirring, cold methyl iodide was added, and the medium was further stirred at room temperature for 1 h. After dilution of the medium with water and acidification, radioactive **4** was extracted with ethyl acetate. Cochromatography with cold compound demonstrated that all the recovered radioactivity (10 μCi) was associated with **4**. The specific activity was 57 000 cpm/nmol.

Photolabeling by 4′-Azido-5-hydroxy-7-[^{14}C]methoxyflavone. A stock solution (5 mM) of the azido chrysin was made in dimethyl sulfoxide. Preliminary experiments in phosphate buffer, pH 6.0, established that the compound was light sensitive, with the absorbance peak at 314 nm becoming less prominent following 1 min of irradiation with the lamp and filters described above. Quantification of $NBD2_{long}$ photolabeling was initially attempted by acid precipitation of the protein following irradiation, collecting the protein on glass fiber filters, and assaying the filters for radioactivity. However, high blanks were encountered. A second method using Ni-chelate chromatography to retain and wash the protein was successful. $NBD2_{long}$ (1 μM) was irradiated in 25 mM MOPS/Tris, pH 7.0, 1 mM EDTA, 20% (w/v) glycerol, and 4′-azido-5-hydroxy-7-[^{14}C]methoxyflavone for 1 min. Urea was added to a concentration of 8 M. The solution was passed over a small column of primed Ni-NTA agarose-25 and the column washed with standard Qiagen buffers followed by a standard elution buffer, all in 8 M urea. An aliquot of the elution buffer was analyzed for radioactivity. Blanks not containing protein were processed at the same time.

RESULTS

Recombinant Polypeptides. The sequences of NBD1 and NBD2 from mouse P-gp are aligned with that of the *Salmonella typhimurium* HisP protein in Figure 1. The limits of the two polypeptides used in this study, namely, Thr^{1044}−Thr^{1224} ($NBD2_{short}$) and Lys^{1025}−Ser^{1276} ($NBD2_{long}$), are indicated, as well as those of the recombinant NBD1 of human P-gp that was found recently to produce Mg^{2+}-dependent $8N_3$-ATP photolabeling (*57*). Our longer polypeptide ($NBD2_{long}$) incorporates all the secondary structural elements of HisP, whereas the shorter one ($NBD2_{short}$) lacks the first β-strand of HisP, including the tyrosine labeled by $8N_3$-ATP in hamster P-gp (*13*), and significant structural elements (three β-strands and three α-helices) on the C-terminal side. The polypeptides were overexpressed in *E. coli* with a $(His)_6$ tag, and purified from the soluble supernatant fraction. Both proteins tended to precipitate in the absence of glycerol and/or high salt concentrations and detergent, the larger one seeming to be more hydrophobic. Therefore, the photolabeling experiments were performed in 20% glycerol and at protein concentrations lower than 0.5 μM.

Photolabeling Characteristics. The photolabeling of $NBD2_{short}$ and $NBD2_{long}$ with $8N_3$-ATP and TNP-$8N_3$-ATP, at pH 6.0 in the presence of EDTA, is shown in parts A and B, respectively, of Figure 2. The photolabeling was saturable with both probes at fairly low concentrations: $K_{0.5}$($8N_3$-ATP) was 36−37 μM for both $NBD2_{short}$ and $NBD2_{long}$, and $K_{0.5}$-(TNP-$8N_3$-ATP) was 0.8 and 2.6 μM, respectively.

The effects of the concentration of salt (NaCl), sucrose, and detergent (Triton X-100) on the photolabeling of $NBD2_{short}$ and $NBD2_{long}$ with TNP-$8N_3$-ATP were investigated (data not shown). High salt concentration (1 M) partially inhibited photolabeling, but in the millimolar range

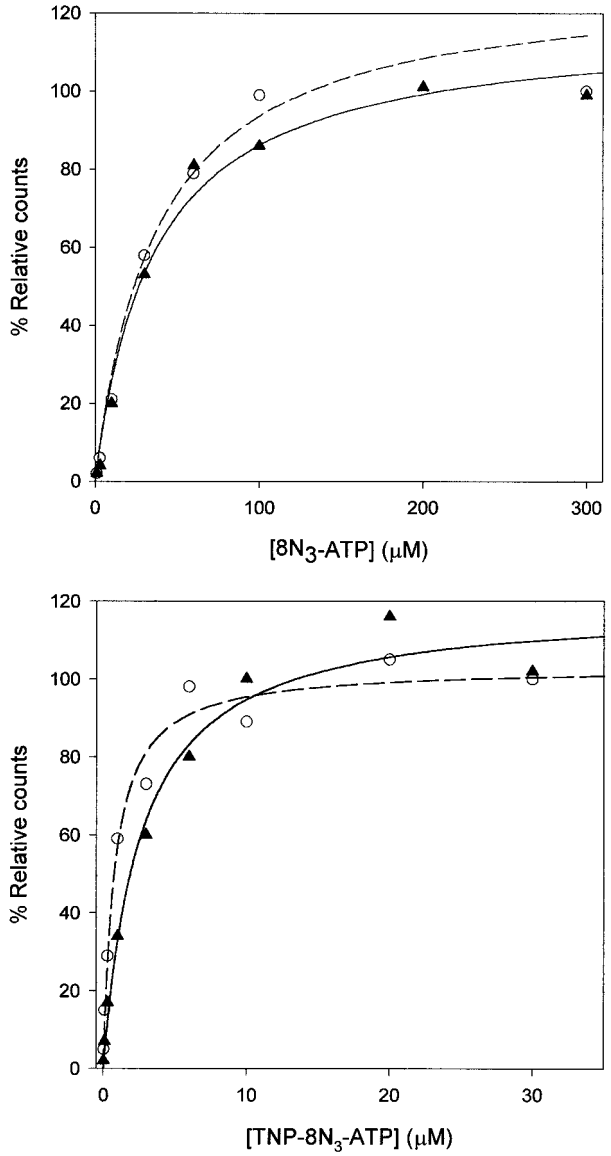

FIGURE 2: Concentration-dependent photolabeling of $NBD2_{short}$ (open symbols) and $NBD2_{long}$ (closed symbols) with $8N_3$-ATP (A, top) and TNP-$8N_3$-ATP (B, bottom). Photolabeling was carried out in the standard medium, with 25 mM MES [2-(*N*-morpholino)-ethanesulfonic acid], pH 6.0, and 2 mM EDTA. The protein concentration was 0.5 or 0.1 μM for [γ-^{32}P]$8N_3$-ATP or [γ-^{32}P]-TNP-$8N_3$-ATP, respectively. The data points at the highest concentration of nucleotide were taken as 100%.

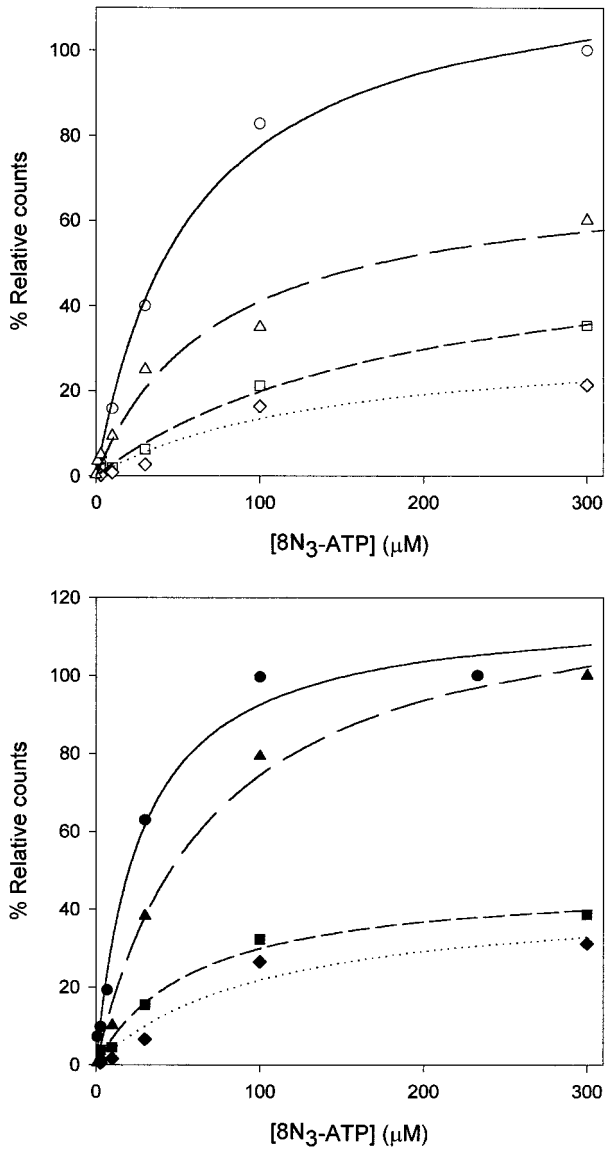

FIGURE 3: Effect of increasing concentrations of $MgCl_2$ on photolabeling of $NBD2_{short}$ (A, top) and $NBD2_{long}$ (B, bottom) with $8N_3$-ATP. Photolabeling was carried out in the standard medium, with 25 mM MES, pH 6.0, including EDTA or $MgCl_2$ as indicated below. The protein concentration was 0.5 μM. The medium contained 10 mM EDTA (circles, solid line), 1 mM $MgCl_2$ (triangles, dashed line), 10 mM $MgCl_2$ (squares, short dashed line), or 30 mM $MgCl_2$ (tilted squares, dotted line). The data points at 300 μM nucleotide in EDTA were taken as 100%.

the effect was small. Sucrose and buffer concentrations had little effect. The effect of detergent was tested by diluting the stock polypeptides (in 0.01% (w/v) HECAMEG) at least 100-fold. Low concentrations of Triton X-100 (above 0.003%) enhanced photolabeling of both NBDs approximately 2-fold, and therefore 0.01% (w/v) Triton X-100 was included in the following standard irradiation medium.

The $MgCl_2$ and pH dependencies of photolabeling are shown in Figures 3 and 4, respectively. For both polypeptides and both probes, $MgCl_2$ had moderate inhibition up to 1 mM, especially for $NBD2_{long}$, and inhibited more strongly at higher concentrations. The inhibition appeared to be due both to decreased efficiency of the photodependent reaction and to decreased affinity for the nucleotide. For example, in the case of $8N_3$-ATP, the $K_{0.5}$($8N_3$-ATP) was raised from 36−37 to 143 and 101 μM for $NBD2_{short}$ and $NBD2_{long}$, respectively, upon addition of 30 mM $MgCl_2$ (Figure 3). Similar results were obtained for TNP-$8N_3$-ATP (data not shown). Photolabeling in the presence of either 1 mM $MgCl_2$ or EDTA was maximal at acidic pH for both probes and polypeptides, and the pH dependence yielded pK_a($8N_3$-ATP) = 6.8−7.4 and pK_a(TNP-$8N_3$-ATP) = 7.5−7.9 (Figure 4).

Since one possibility for such a pH dependence might be hydrolysis of the γ-phosphate of the probe or instability of the probe/protein attachment at alkaline pH. This was tested by photolabeling $NBD2_{short}$ and $NBD2_{long}$ with [γ-^{32}P]TNP-$8N_3$-ATP at pH 6.0 with or without 1 mM Mg^{2+}, and monitoring the radioactivity remaining with the protein over 1 h at 25 °C. However, the level of radioactivity monitored by SDS−PAGE and instant imaging was not dependent on the time of incubation or the conditions.

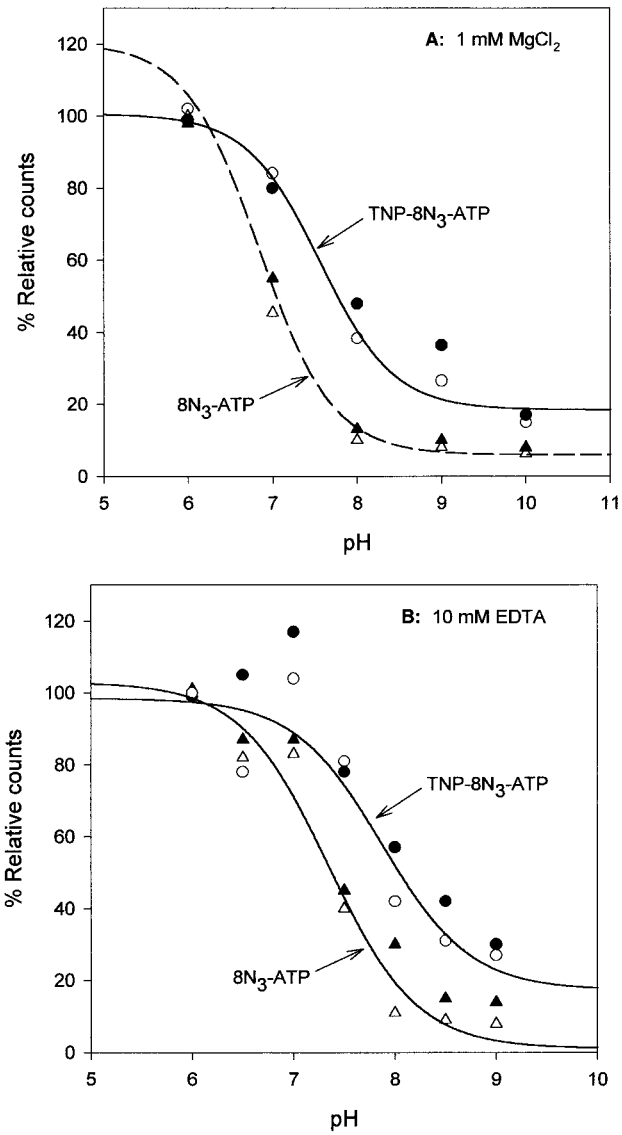

FIGURE 4: pH-dependent photolabeling of $NBD2_{short}$ (open symbols) and $NBD2_{long}$ (closed symbols) with $8N_3$-ATP (triangles) and TNP-$8N_3$-ATP (circles). Photolabeling was carried out in the standard medium containing either 1 mM $MgCl_2$ (A, top) or 10 mM EDTA (B, bottom). MES was used as buffer at pH 6.0 or 6.5, HEPES [*N*-(2-hydroxyethyl)piperazine-*N*′-(2-ethanesulfonic acid)] at pH 7.0 or 7.5, EPPS [*N*-(2-hydroxyethyl)piperazine-*N*′-(3-propanesulfonic acid)] at pH 8.0 or 8.5, and CHES [2-(*N*-cyclohexylamino)-ethanesulfonic acid] at pH 9.0 or 10.0. The protein concentration was 0.5 and 0.1 μM for [γ-^{32}P]$8N_3$-ATP and [γ-^{32}P]TNP-$8N_3$-ATP, respectively. The curves shown are the best fits to $NBD2_{short}$ data photolabeled with [γ-^{32}P]$8N_3$-ATP (dashed line) and [γ-^{32}P]TNP-$8N_3$-ATP (solid line). The data points at pH 6.0 were taken as 100%.

The efficiency of photolabeling was determined under optimal conditions by either of the two following methods. The first one involved acid precipitation of the derivatized protein, recovery of the protein on glass fiber filters, and counting of the radioactivity. The second one used SDS−PAGE and quantification by instant imaging with reference to a standard amount of $^{32}P[P_i]$ incorporated into the gel on a small piece of filter paper. At a concentration of nucleotide of $3K_{0.5}$ (corresponding to 75% saturation) and pH 6.0 in the absence of Mg^{2+}, the level of derivatization using both methods was approximately 0.5 mol/mol of NBD2 for both probes and both polypeptides (range for different preparations 0.2−0.7 mol/mol). This means that the efficiency of derivatization at saturation is on average close to 0.7 mol/mol of NBD2.

Nucleotide Inhibition of Photolabeling. The effect of increasing concentrations of ATP and TNP-ATP on the photolabeling of the polypeptides in the presence of EDTA is shown in Figure 5. Both nucleotides almost completely inhibited the photolabeling of both polypeptides, in a monophasic manner indicative of a single class of sites. The derived "true" affinities, assuming close-to-equilibrium conditions, are the following:

for $8N_3$-ATP

$NBD2_{short}$: K_D(TNP-ATP) = 0.1 μM, K_D(ATP) = 1 mM

$NBD2_{long}$: K_D(TNP-ATP) = 0.6 μM, K_D(ATP) = 0.5 mM

for TNP-$8N_3$-ATP

$NBD2_{short}$: K_D(TNP-ATP) = 0.5 μM, K_D(ATP) = 1.7 mM

$NBD2_{long}$: K_D(TNP-ATP) = 5.0 μM, K_D(ATP) = 2.7 mM

The discrepancies between photoprobes are most probably due to conditions deviating from equilibrium.

Flavonoid Inhibition of Photolabeling. To identify, on one hand, functionalities on the flavonoid nucleus which are important for binding to the ATP site and, on the other hand, positions on the nucleus where substitution may be possible, the effect of a variety of flavonoids was tested on photolabeling. The basic structures of the different classes of flavonoids investigated in this study are shown in Figure 6, and the 30 compounds used are listed in Table 1. The compounds were screened at 50 μM for inhibition of photolabeling of $NBD2_{long}$ by a photoprobe concentration equal to $K_{0.5}$, in a medium containing 10 mM EDTA at pH 6.0. Among the 30 compounds tested, only kaempferide, galangin, dehydrosilybin, and broussochalcone A inhibited photolabeling. The concentration-dependent inhibition of $NBD2_{long}$ photolabeling by TNP-$8N_3$-ATP is shown in Figure 7 and yielded K_D(kaempferide) = 1.9 μM, K_D(galangin) = 20 μM, K_D(dehydrosilybin) = 32 μM, and K_D(broussochalcone A) = 11 μM. These flavonoids were also the only ones that inhibited photolabeling by $8N_3$-ATP (results not shown). While kaempferide itself binds fairly tightly to the ATP site, hydrophobic substitutions on the 8-position prevent binding. Galangin, which is not substituted at position 4′, binds well, whereas extensions at either position 8 or position 6 also prevent binding. Chrysin and derivatives, all of which lack the 3-OH, cannot bind to the ATP site. The only direction in which extensions are permitted seems to be on ring B, as demonstrated by the binding of dehydrosilybin. Furthermore, the double bond between carbons 2 and 3 on ring C appears to be essential for ATP site recognition as silybin itself shows no inhibition of photolabeling.

The binding of flavonoids to NBD_{short} has been previously measured using tryptophan fluorescence quenching (*39*, *44*−*48*), and the obtained K_D values are listed in Table 1. The K_D for kaempferide is similar to that found in this study, but the values for galangin and broussochalcone A are tighter.

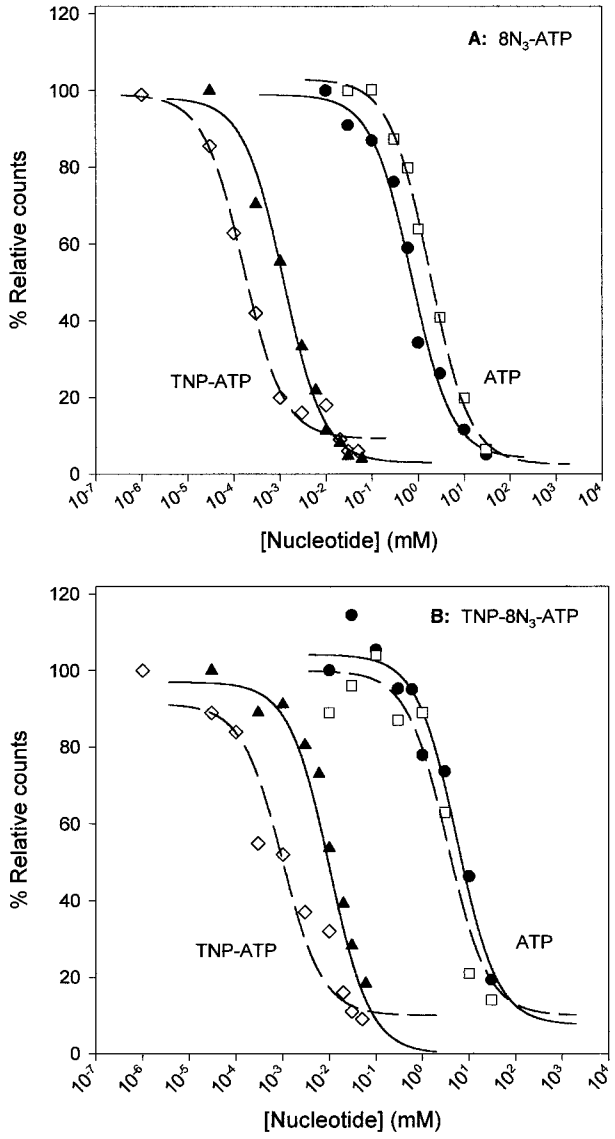

FIGURE 5: Nucleotide inhibition of $NBD2_{short}$ (open symbols) and $NBD2_{long}$ (closed symbols) photolabeling by $8N_3$-ATP (A, top) or TNP-$8N_3$-ATP (B, bottom). Photolabeling was carried out in the standard medium including 10 mM EDTA. The concentrations of [γ-^{32}P]$8N_3$-ATP and [γ-^{32}P]TNP-$8N_3$-ATP were equal to $K_{0.5}$ (see Figure 2), and the protein concentrations were 0.5 and 0.1 μM for the two probes, respectively. Data obtained in the absence of TNP-ATP and ATP were taken as 100%. Circles, solid line: $NBD2_{long}$, photolabeling inhibited with ATP. Triangles, solid line: $NBD2_{long}$, photolabeling inhibited with TNP-ATP. Open squares, dashed line: $NBD2_{short}$, photolabeling inhibited with ATP. Open tilted squares, dashed line: $NBD2_{short}$, photolabeling inhibited with TNP-ATP.

Interestingly, several chrysin hydrophobic derivatives have been found to bind extremely tightly (*48*) and yet do not inhibit photolabeling; they evidently do not bind to the ATP site.

Photolabeling with 4′-Azido-5-hydroxy-7-[^{14}C]methoxyflavone. The very tight binding of several chrysins to $NBD2_{short}$ prompted us to synthesize a radiolabeled azido derivative to localize the binding site in the structure. However, irradiation under conditions under which tight binding of the chrysins has been found and under which most of the probe is photolyzed failed to derivatize the protein significantly.

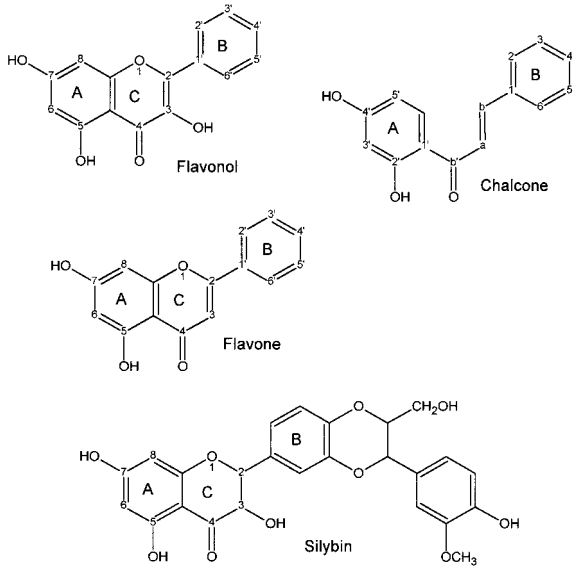

FIGURE 6: Basic structures of the different classes of flavonoids: galangin (flavonol), chalcone, chrysin (flavone), and silybin.

DISCUSSION

The present work has shown that $8N_3$-ATP and TNP-$8N_3$-ATP photolabel two different sizes of recombinantly expressed NBD2 of mouse P-gp with nearly stoichiometric derivatization at acidic pH. The apparent tight binding of the TNP nucleotide is consistent with the much higher affinity for TNP-ATP as compared with ATP exhibited by both the whole P-gp and the recombinant NBDs (*10*−*12*, *58*, *59*). The strong inhibition of photolabeling by TNP-ATP and ATP is also indicative of a properly constituted ATP site. The atomic structures of HisP (*56*), ArsA (*60*), and Rad50 (*7*) ATPases all indicate that the ribose hydroxyls of bound nucleotide are not enclosed by protein, and evidently a TNP moiety can be accommodated in this position.

Mg^{2+} in the submillimolar concentration range does not markedly affect photolabeling, especially in the case of $NBD2_{long}$, but strongly inhibits at high concentrations. Photolabeling of human P-gp and of several whole yeast ABC multidrug transporters have been found to be highly dependent on Mg^{2+} (*17*, *61*, *62*). Photolabeling of recombinant soluble human NBD1 is Mg^{2+} dependent if the size of the polypeptide is above a certain minimum, with important determinants on both the N- and C-terminal sides (*57*). The critical length is very similar to that of our $NBD2_{long}$ polypeptide, although a small segment is missing on the N-terminal end (cf. Figure 1). Since the latter portion is not unduly conserved among P-gp's, it is possible that NBD1 and NBD2 may differ with respect to the minimum requirements that constitute a Mg^{2+} site. The recent structures of Rad50 and ArsA ATPases suggest that the two MgATP sites form at the interface of a dimeric interaction between the two NBDs (*7*, *60*). Thus, interaction between NBD1 and NBD2 may be required for proper reconstitution of the MgATP site of recombinant soluble NBD2 and for yielding a Mg^{2+} dependence of photolabeling. In this respect, it is interesting that, in whole human P-gp and in the related multidrug resistance associated protein (MRP1) when expressed as two half-molecules, $8N_3$-ATP preferentially photolabels NBD1 while trapping of $8N_3$-ADP with vanadate occurs at NBD2 (*61*, *63*). In the case of MRP1, recombi-

Table 1: Flavonoids Investigated in This Study, with Corresponding Dissociation Constants Previously Determined on Recombinant Soluble $NBD2_{short}$ by Quenching of Intrinsic Tryptophan Fluorescence (*39*, *44*−*48*)

flavonol	substituents 3	6	8	4′	K_D (μM)
galangin	OH				5.3
6-prenylgalangin	OH	Pre			0.21
8-prenylgalangin	OH	Pre			0.22
kaempferide	OH			OCH_3	4.5
8-(1,1-DMA)kaempferide	OH		DMA	OCH_3	0.20
8-(1,1-DMA)-3-methylkaempferide	OCH_3		DMA	OCH_3	0.12

chalcone	substituents 5′	3	4	K_D (μM)
broussochalcone A	Pre	OH	OH	0.44
4-C_2H_5-chalcone			C_2H_5	2.1
4-C_4H_9-chalcone			C_4H_9	1.0
4-C_6H_{13}-chalcone			C_6H_{13}	0.27
4-C_8H_{17}-chalcone			C_8H_{17}	0.02
4-F-chalcone			F	3.6
4-I-chalcone			I	0.25
4-OH-chalcone		OH	OH	4.8
4-OH-3-prenylchalcone		Pre	OH	0.53

flavone	substituents 6	7	8	4′	K_D (μM)
chrysin					13.1
6-prenylchrysin	Pre				0.30
7-prenylchrysin		Pre			0.045
tectochrysin		OCH_3			6.3
8-(1,1-DMA)chrysin			DMA		0.20
8-prenylchrysin			Pre		0.28
6,8-diprenylchrysin	Pre		Pre		0.015
6-geranylchrysin	Ger				0.045
8-geranylchrysin			Ger		0.025
4′-F-chrysin				F	2.7
4′-I-chrysin				I	2.2

silybin derivative	substituents 2 and 3	6	8	K_D (μM)
silybin				6.8
dehydrosilybin	double bond			2.2
6-prenyldehydrosilybin		Pre		0.37
8-prenyldehydrosilybin			Pre	0.25

nantly expressed NBD1, but not NBD2, could be photolabeled.

The pH dependence of photolabeling indicates that protonation of ionizable group(s), with a pK_a of 6.8 for $8N_3$-ATP or 7.5−7.8 for TNP-$8N_3$-ATP, aids nitrene insertion into the protein. In the absence of Mg^{2+}, this could be attributable to protonation of the γ-phosphate with a pK_a-(ATP) of 6.8 (*64*). But this explanation seems to be incompatible with the finding that 1 mM Mg^{2+} has no effect on the pK_a of photolabeling, since MgATP does not ionize in this pH range. It seems doubtful that the 8-azido derivative would be different in this respect. An alternative explanation is that the polypeptide itself, perhaps at the ATP site, might ionize in this range, modulating either nucleotide binding or the photochemical reaction. It is also possible that the folding of the fragments or stability of the folded structures is pH dependent.

A surprising aspect of our results is that $NBD2_{short}$, which lacks the first central β-strand of the HisP structure (*56*), including the conserved tyrosine photolabeled in hamster P-gp by $8N_3$-ATP (*13*), and further structural elements on the C-terminal side is efficiently photolabeled, similar to the longer domain. These findings suggest that an ATP site is constituted from quite a small core of structural elements. It may just include the two β-strands leading into the P-loop of the Walker A motif, the P-loop itself, and the following helix, over which the nucleotide is positioned in the HisP, RbsA (*65*), ArsA, and Rad50 ATPase structure. Therefore, the tyrosine photolabeled in the whole hamster P-gp might not contribute significant binding energy to the $8N_3$-ATP/protein interaction in mouse NBD2, although it could do so for ATP itself. The result also implies the existence of alternative target residue(s) for the reactive nitrene besides the tyrosine. Consideration of the crystal structures of ABC ATPases suggests several possibilities, including a tyrosine in the aforementioned helix, which interacts with the adenine of bound ATP in the ribose transporter RbsA (*65*). Despite considerable effort, so far we have been unable to identify the amino acid residue(s) photolabeled with TNP-$8N_3$-ATP, and this suggests that derivatization may not be confined to a single residue within the ATP site. The binding energy may derive largely from the phosphate/protein interaction, leaving the adenyl moiety rather mobile, as recently found in the maltose transporter MalK (*66*). TNP-AMP, in contrast to TNP-ATP and TNP-ADP, has been reported to bind poorly to full-length human P-gp (*58*). Aromatic residues in the ATP site of the related cystic fibrosis transmembrane conductance regulator do not contribute to nucleotide binding interactions, also suggesting that the phosphate/protein interactions may dominate binding (*67*). Therefore, despite some minor differences, both lengths of NBD2 are suited for monitoring binding to, and photolabeling of, the P-gp ATP site.

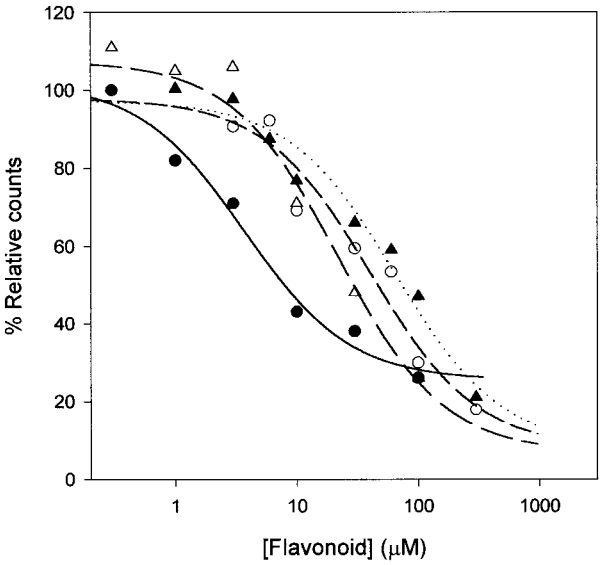

FIGURE 7: Flavonoid inhibition of TNP-$8N_3$-ATP photolabeling of $NBD2_{long}$. Photolabeling was carried out in the standard medium including 10 mM EDTA. The concentration of [γ-^{32}P]TNP-$8N_3$-ATP was equal to $K_{0.5}$, and the protein concentration was 0.1 μM. Data obtained in the absence of flavonoid were taken as 100%. Filled circles, solid line: kaempferide. Open triangles, medium dashed line: broussochalcone A. Open circles, short dashed line: galangin. Filled triangles, dotted line: dehydrosilybin.

Flavonoids constitute a large and diverse pool of plant metabolites that offer potential as multidrug resistance reversers and serve as a useful scaffold to drug diversity. Only 4 out of 30 screened, namely, kaempferide, galangin, dehydrosilybin, and broussochalcone A, inhibited photo-

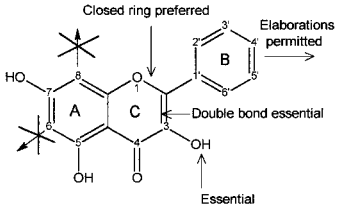

FIGURE 8: Summary of the requirements for flavonoid binding to the ATP site of NBD2. X's indicate nonpermitted extensions.

labeling in the low micromolar range. The tight binding of kaempferide and galangin measured by protection against photolabeling is consistent with previous tight binding to recombinant soluble NBD_{short} measured directly by quenching of intrinsic tryptophan fluorescence (*39*). A simple and consistent picture emerges from the present analysis, in which the basic flavonol nucleus, as exemplified by galangin (Figure 8), fits snugly into the ATP site. Hydrophobic substitutions on the 6 and 8 positions of ring A are not tolerated. The 3-OH group on ring C contacts the protein favorably as the chrysin derivatives, which lack this group, do not bind. A direct role for the 3-OH group was also found in the crystal structure of the Hck tyrosine kinase (*68*). The only direction in which extensions are permitted here for P-gp NBD2 is on ring B, as exemplified by kaempferide itself (with a methoxy group) and dehydrosilybin (with a monolignol unit). In fact, the binding of the latter shows that large extensions are possible in this direction. The aromatic character of ring C of the benzopyrone moiety is important as silybin (with a reduced 2,3-bond) does not bind. Broussochalcone A appears at first sight to be the odd one out, since (i) it lacks the hydroxyl at the 3 position (flavonol numbering) and (ii) it bears a hydrophobic dimethylallyl substituent on ring A. However, since the opening of ring C brings much greater flexibility to the molecule, it might be hypothesized that this molecule binds back to front, in such a way that ring A with the dimethylallyl substituent might be positioned where ring B of the flavonol normally is, and reciprocally ring B at the ring A site. As mentioned above, the structures of the nucleotide-binding sites of the ABC ATPases determined to date indicate that the only possible direction for nucleotide substitution is from the ribose hydroxyls. This means that ring B of the flavonoid nucleus most probably binds at the ribose site. This in turn places rings A and C at the adenine site, which is compatible with their similar sizes and the need for aromaticity in the flavonoid nucleus, as also found for the crystal structures of Hck tyrosine kinase (*68*) and cyclin-dependent protein kinase 2 (*69*).

Finally, several of the hydrophobic chrysin derivatives used in this study, which bind extremely tightly to NBD2 (*48*), however do not inhibit photolabeling of the ATP site. This points to the presence of another flavonoid-binding site on NBD2, which may offer possibilities as an inhibitor- or reverser-binding site since 8-prenylchrysin is indeed able to inhibit P-gp and to induce intracellular daunomycin accumulation in MDR leukemic cells (*48*). A hydrophobic steroid-binding site, distinct from the ATP site, has been found in both recombinant NBD1 (*70*) and NBD2 (*39*) of mouse P-gp, and in NBD2 of the *L. tropica* P-gp-like transporter (*40*). Furthermore, flavonoids inhibit competitively and more strongly the energy-dependent interaction of rhodamine 6G than ATPase activity in the case of the yeast Pdr5p transporter (*41*). Also the fact that radioactive 4′-azido-5-hydroxy-7-methoxyflavone failed to photolabel NBD2 supports the existence of a second hydrophobic binding site for flavonoids. A hydrophobic binding site can be expected to be poorly derivatized by an aryl azido, as the photoactivated nitrene is known to only react efficiently with nucleophiles present in polar amino acid side chains (*71*). Binding of 4′-azido-5,7-dihydroxyflavone, a representative of the flavone class, is likely to be directed to the alternate hydrophobic binding site lacking reactive amino acid side chains, rather than to the ATP site.

ACKNOWLEDGMENT

We thank Peggy Mobo and David Woolley for their expert technical assistance.

REFERENCES

1. Ling, V. (1992) *Cancer 69*, 2603−2609.
2. Gottesman, M. M., and Pastan, I. (1993) *Annu. Rev. Biochem. 62*, 385−427.
3. Liu, R., and Sharom, F. J. (1998) *Biochemistry 37*, 6503−6512.
4. van Veen, H. W., and Konings, W. N. (1998) *Biochim. Biophys. Acta 1365*, 31−36.
5. Walker, J. E., Saraste, M., Runswich, M. J., and Gay, N. J. (1982) *EMBO J. 1*, 945−951.
6. Ames, G. F.-L., Mimura, C. S., Holbrook, S. R., and Shyamala, V. (1992) *Adv. Enzymol. Relat. Areas Mol. Biol. 65*, 1−47.
7. Hopfner, K. P., Karcher, A., Shin, D. S., Craig, L., Arthur, L. M., Carney, J. P., and Tainer, J. A. (2000) *Cell 101*, 789−800.
8. Al-Shawi, M. K., Urbatsch, I. L., and Senior, A. E. (1994) *J. Biol. Chem. 269*, 8986−8992.
9. Beaudet, L., Urbatsch, I. L., and Gros, P. (1998) *Biochemistry* 37, 9073−9082.
10. Baubichon-Cortay, H., Baggetto, L. G., Dayan, G., and Di Pietro, A. (1994). *J. Biol. Chem. 269*, 22983−22989.
11. Senior A. E., Al-Shawi, M. K., and Urbatsch, I. L. (1995) *J. Bioenerg. Biomembr. 27*, 31−36.
12. Dayan, G., Baubichon-Cortay, H., Jault, J.-M., Cortay, J.-C., Deleage, G., and Di Pietro, A. (1996) *J. Biol. Chem. 271*, 11652−11658.
13. Sankaran, B., Bhagat, S., and Senior, A. E. (1997) *FEBS Lett. 417*, 119−122.
14. Loo, T. W., and Clarke, D. M. (1995) *J. Biol. Chem. 270*, 22957−22961.
15. Urbatsch, I. L., Sankaran, B., Weber, J., and Senior, A. E. (1995) *J. Biol. Chem. 270*, 19383−19390.
16. Liu, R., and Sharom F. J. (1996) *Biochemistry 35*, 11865−11873.
17. Hrycyna, C. A., Ramachandra, M., Ambudkar, S. V., Ko, Y. H., Pedersen, P. L., Pastan, I., and Gottesman, M. M. (1998) *J. Biol. Chem. 273*, 16631−16634.
18. Takada, Y., Yamada, K., Taguchi, Y., Kino, K., Matsuo, M., Tucher, S., Komano, T., Amachi, T., and Ueda, K. (1998) *Biochim. Biophys. Acta 1374*, 131−136.
19. Senior, A. E., and Bhagat, S. (1998) *Biochemistry 37*, 831−836.
20. Urbatsch, I. L., Beaudet, L., Carrier, I., and Gros, P. (1998) *Biochemistry 37*, 4592−4602.
21. Safa, A. R., Stern, R. K., Choi, K., Agresti, M., Tamai, I., Mehta, N. D., and Roninson I. B. (1990) *Proc. Natl. Acad. Sci. U.S.A. 87*, 7225−7229.
22. Greenberger, L. M., Sisanti, C. J., Silva, J. T., and Horwitz, S. B. (1991) *J. Biol. Chem. 266*, 20744−20751.
23. Greenberger, L. M. (1993) *J. Biol. Chem. 268*, 11417−11425.
24. Kajiji, S., Talbot, F., Grizzuti, K., Van Dyke-Phillips, V., Agresti, M., Safa, A. R., and Gros, P. (1993) *Biochemistry 32*, 4185−4194.

25. Loo, T. W., and Clarke, D. M. (1994) *Biochemistry 33*, 14049−14057.
26. Zhang, X., Collings, K. I., and Greenberger, L. M. (1995) *J. Biol. Chem. 270*, 5441−5448.
27. Loo, T. W., and Clarke, D. M. (1997) *J. Biol. Chem. 272*, 31945−31948.
28. Taguchi, Y., Kino, K., Morishima, M., Komano, T., Kane, S. E., and Ueda, K. (1997) *Biochemistry 36*, 8883−8889.
29. Demeule, M., Laplante, A., Murphy, G. F., Wenger, R. M., and Beliveau, R. (1998) *Biochemistry 37*, 18110−18118.
30. Vo, Q. D., and Gruol, D. J. (1999) *J. Biol. Chem. 274*, 20318−20327.
31. Boer, R., Dichtl, M., Borchers, C., Ulrich, W. R., Marecek, J. F., Prestwich, G. D., Glossmann, H., and Striessnig, J. (1996) *Biochemistry 35*, 1387−1396.
32. Garrigos, M., Mir, L. M., and Orlowski, S. (1997) *Eur. J. Biochem. 244*, 664−673.
33. Callaghan, R., Berridge, G., Ferry, D. R., and Higgins, C. F. (1997) *Biochim. Biophys. Acta 1328*, 109−124.
34. Phang, J. M., Poore, C. M., Lopaczynska, J., and Yeh, G. C. (1993) *Cancer Res. 53*, 5977−5981.
35. Scambia, G., Ranelletti, F. O., Panici, P. B., De Vincenzo, R., Bonanno, G., Ferrandina, G., Piantelli, M., Bussa, S., Rumi, C., and Cianfriglia, M. (1994) *Cancer Chemother. Pharmacol. 34*, 459−464.
36. Castro, A. F., and Altenberg, G. A. (1997) *Biochem. Pharmacol. 53*, 89−93.
37. Ferte, J., Kuhnel, J.-M., Chapuis, G., Rolland, Y., Lewin, G., and Schwaller, M. A. (1999) *J. Med. Chem. 42*, 478−489.
38. Loo T. W., and Clarke, D. M. (1994) *J. Biol. Chem. 269*, 7750−7755.
39. Conseil, G., Baubichon-Cortay, H., Dayan, G., Jault, J.-M., Barron, D., and Di Pietro, A. (1998) *Proc. Natl. Acad. Sci. U.S.A. 95*, 9831−9836.
40. Perez-Victoria, J. M., Chiquero, M. J., Conseil, G., Dayan, G., Di Pietro, A., Barron, D., Castanys, S., and Gamarro, F. (1999) *Biochemistry 38*, 1736−1743.
41. Conseil, G., Decottignies, A., Jault, J.-M., Comte, G., Barron, D., Goffeau, A., and Di Pietro, A. (2000) *Biochemistry 39*, 6910−6917.
42. Hiratsuka, T. (1982) *Biochim. Biophys. Acta 719*, 509−517.
43. Noungoue-Tchamo, D., Barron, D., and Mariotte, A.-M. (1995) *Nat. Prod. Lett. 7*, 73−80.
44. Bois, F., Beney, C., Boumendjel, A., Mariotte, A.-M., Conseil, G., and Di Pietro, A. (1998) *J. Med. Chem. 41*, 4161−4164.
45. Bois F., Boumendjel A., Mariotte A.-M., Conseil, G., and Di Pietro A. (1999) *Bioorg. Med. Chem. 7*, 2691−2695..
46. Daskiewicz, J.-B., Comte, G., Barron, D., Di Pietro, A., and Thomasson, F. (1999) *Tetrahedron Lett. 40*, 7095−7098.
47. Maitrejean, M., Comte, G., Barron, D., El Kirat, K., Conseil, G., and Di Pietro, A. (2000) *Bioorg. Med. Chem. Lett. 10*, 157−160.
48. Comte, G., Daskiewicz, J.-B., Bayet, C., Conseil, G., Viornery-Vanier, A., Dumontet, C., Di Pietro, A., and Barron, D. (2001) *J. Med. Chem. 44*, 763−768..
49. Laemmli, U. K. (1970) *Nature 227*, 680−685.
50. Seebregts, C. J., and McIntosh, D. B. (1989) *J. Biol. Chem. 264*, 2043−2052.
51. Glynn, I. M., and Chappell, J. B. (1964) *Biochem. J. 90*, 147−149.
52. McIntosh, D. B., Woolley, D. G., and Berman, M. C. (1992) *J. Biol. Chem. 267*, 5301−5309.
53. Cushman, M., and Nagarathnam, D. (1990) *Tetrahedron Lett. 31*, 6497−6500.
54. Ram, S., and Ehrenkaufer, A. E. (1984) *Tetrahedron Lett. 25*, 3415−3418.
55. Cunningham, B. D., Threadgill, M. D., Groundwater, P. W., Dale, I. L., and Hickman, J. A. (1992) *Anti-Cancer Drug Des. 7*, 365−384.
56. Hung L.-W., Wang, I. X., Nikaido, K., Liu, P.-Q., Ames G, F.-L., and Kim, S.-H. (1998) *Nature 396*, 703−707.
57. Booth, C. L., Pulaski, L., Gottesman, M. M., and Pastan, I. (2000) *Biochemistry 39*, 5518−5526.
58. Liu, R., and Sharom, F. J. (1997) *Biochemistry 36*, 2836−2843.
59. Lerner-Marmarosh, N., Gimi, K., Urbatsch, I. L., Gros, P., and Senior, A. E. (1999) *J. Biol. Chem. 274*, 34711−34718.
60. Zhou, T., Radaev, S., Rosen, B. P., and Gatti, D. L. (2000) *EMBO J. 19*, 4838−4845.
61. Hrycyna, C. A., Ramachandra, M., Germann, U. A., Cheng, P. U., Pastan, I., and Gottesman, M. M. (1999) *Biochemistry 38*, 13887−113899.
62. de Wet, H. (2000) Ph.D. Thesis, University of Cape Town, South Africa.
63. Gao, M., Cui, H. R., Loe, D. W., Grant, C. E., Almquist, K. C., Cole, S. P. C., and Deeley, R. G. (2000) *J. Biol. Chem. 275*, 13098−13108.
64. Pecoraro, V. l., Hermes, J. D., and Cleland, W. W. (1984) *Biochemistry 22*, 5262−5271.
65. Armstrong, S., Tabernero, L., Zhang, H., Hermoden, M., and Stauffacher, P. (1988) *Pediatr. Pulmonol. 17*, 91−92.
66. Diederichs, K., Diez, J., Greller, G., Müller, C., Breed, J., Schnell, C., Vonfhein, C., Boos, W., and Welte, W. (2000) *EMBO J. 19*, 5951−5961.
67. Berger, A. L., and Welsh, M. J. (2000) *J. Biol. Chem. 275*, 26407−29412.
68. Sicheri, F., Moarefi, I., and Kurijan, J. (1997) *Nature 385*, 602−609.
69. De Azevedo, W. F., Jr., Mueller-Dieckmann, H.-J., Schulze-Gahmen, U., Worland, P. J., Sausville, E., and Kim, S.-H. (1996) *Proc. Natl. Acad. Sci. U.S.A. 93*, 2735−2740.
70. Dayan, G., Jault, J.-M., Baubichon-Cortay, H., Baggetto, L. G., Renoir, J.-M., Baulieu, E. E., Gros, P., and Di Pietro, A. (1997) *Biochemistry 36*, 15208−15215.
71. Kotzyba-Hibert, F., Kapfer, I., and Goeldner, M. (1995) *Angew. Chem., Int. Ed. Engl. 34*, 1296−1312.

BI010657C